DISCRETE AND CONTINUOUS
DYNAMICAL SYSTEMS
Volume **9**, Number **3**, May **2003**

Website: http://AIMsciences.org

pp. **559–576**

EVOLUTION GALERKIN SCHEMES APPLIED TO TWO-DIMENSIONAL RIEMANN PROBLEMS FOR THE WAVE EQUATION SYSTEM

Jiequan Li
Department of Mathematics, Captial Normal University,Beijing, China

Mária Lukáčová - Medviďová
Arbeitsbereich Mathematik, Technische Universität Hamburg-Harburg
Hamburg, Germany
and
Gerald Warnecke
Institut für Analysis und Numerik, Otto-von-Guericke-Universität Magdeburg
Magdeburg, Germany

(Communicated by Fanghua Lin)

Abstract. The subject of this paper is a demonstration of the accuracy and robustness of evolution Galerkin schemes applied to two-dimensional Riemann problems with finitely many constant states. In order to have a test case with known exact solution we consider a linear first order system for the wave equation and test evolution Galerkin methods as well as other commonly used schemes with respect to their accuracy in capturing important structural phenomena of the solution. For the two-dimensional Riemann problems with finitely many constant states some parts of the exact solution are constructed in the following three steps. Using a self-similar transformation we solve the Riemann problem outside a neighborhood of the origin and then work inwards. Next a Goursant-type problem has to be solved to describe the interaction of waves up to the sonic circle. Inside it a system of composite elliptic-hyperbolic type is obtained, which may not always be solvable exactly. There an interesting local maximum principle can be shown. Finally, an exact partial solution is used for numerical comparisons.

1. **Introduction.** This paper is concerned with the accuracy of numerical approximations for solutions to systems of hyperbolic conservation laws. In order to precisely assess the accuracy of numerical schemes it is of fundamental importance to have a wide range of different exact solutions. Only in such cases one can determine the exact error of the approximation. For multidimensional systems of partial differential equations this is quite a challenge.

One commonly used possibility to design such test cases for smooth solutions is to take some simple, e.g. polynomial, trigonometric or exponential, functions. One may insert them into the differential part of the equations and then adjust the right hand side as well as the data in order to obtain a solution, see e.g. Lukáčová *et al.*

1991 *Mathematics Subject Classification.* 35L05, 65M06, 35L45, 35L65, 65M25, 65M15.

Key words and phrases. genuinely multidimensional schemes, hyperbolic systems, wave equation, Euler equations, evolution Galerkin schemes, Riemann problem.

This research was supported under the DFG grant No. Wa 633/6-2 of Deutsche Forschungsgemeinschaft, the Volkswagen Stiftung and partially by the GIF German-Israeli Foundation grant I-318-195.06/93 as well as by the grants CZ 39001/2201 and GAČR 201/00/0557 of the Czech Grant Agency.

[17]. This is quite nice for a start, but it is difficult to assess special properties of schemes in general applications, since these solutions are quite special and possibly unrealistic for true applications.

In designing schemes for conservation laws it is important to study discontinuous solutions. Numerical difficulties at contact discontinuities in nonlinear systems like the Euler equations of gas dynamics are quite well known. Therefore, it is useful to study discontinuous solutions to the two-dimensional Riemann problem for linear systems as a first step. The aim is to obtain as much exact information on the solution of test cases as possible in order to calculate the local error of the scheme. This will be done in this paper by considering a 3 by 3 linear system for the wave equation that is related to the linearized accoustic part of the Euler equations.

The two-dimensional Riemann problem is given by initial data which consist of piecewise constant states on a finite number of sectors going out from the origin of the plane. A common simple example is to take four quadrants obliquely to the mesh. The solution at a later time consists basically of two main parts. In a small region around the origin, i.e. inside the sonic circle, it has a complicated structure that is obtained as a solution to an elliptic boundary value problem. This part of the solution is not known exactly. Outside this region the solution is piecewise constant and the location of the discontinuities between these states is known exactly.

Another important issue for test cases is to obtain as much qualitative information on the specific, e.g. monotonicity or maximum principle type properties, in those local parts of the solution where it is not known exactly. One may then test the scheme for the preservation of such properties.

The structure of the paper is as follows. First we study the solution near infinity by making use of its self-similarity. We obtain a time-independent system in two variables and demonstrate its solvability. This solution may be extended inwards to a certain region. Then we have to solve a Goursat-type problem with possibly discountinuous boundary values to go further inward. Next, we study the boundary value problem for the extension of the solution to the remaining neighborhood of the origin. We prove the solvability of this problem using the theory of symmetric positive systems due to Friedrichs [8]. We also prove a maximum principle that should be respected by numerical approximations.

In the remaining parts of the paper we give explicitly the construction of parts of the solution for an example that we use to compare various schemes. We are developing evolution Galerkin (EG) type schemes using the bicharacteristic cones of the system in their construction specifically to deal with multidimensional solution features. Variants of these second order schemes based on a finite volume formulation are applied to this test case. Comparisons with a scheme of Butler, a finite volume flux vector splitting scheme and the rotated Richtmyer Lax-Wendroff scheme are made.

The study of the error in local parts of solutions to multidimensional Riemann problems may be extended also to nonlinear systems. The analysis becomes quite a bit more involved. Results of the kind that would be needed may be found in Li *et al.* [15]. Since such solutions have been used as numerical test cases in recent years, see e.g. Schulz-Rinne [26], it would be important to extend the results in this paper to some of the test cases already in use.

2. **Construction of two-dimensional Riemann solutions.**

In this section we construct explicitly Riemann solutions of the two dimensional Riemann problem

for wave equation system

$$\begin{cases} \phi_t + c(u_x + v_y) = 0 \\ u_t + c\phi_x = 0 \\ v_t + c\phi_y = 0 \end{cases} \tag{2.1}$$

subject to the initial data

$$(\phi, u, v)(t = 0, x, y) = (\phi_0, u_0, v_0)(\theta), \tag{2.2}$$

where $0 \le \theta < 2\pi$ is the polar angle. For the purpose of numerical experiments, (ϕ_0, u_0, v_0) is restricted to be a finite number of constant states, being discontinuous along rays through the origin.

As the initial data are discontinuous, the solution of (2.1) and (2.2) must be discontinuous and discontinuities propagate along characteristics by the well–known theory of hyperbolic systems. Therefore (2.1) and (2.2) must be understood in $L^\infty(\mathbb{R}^3_+)$, see [27].

We prove by a construction that the solution is in L^∞. Now we try to find out how to construct the explicit solution. For this purpose, we need to understand how the discontinuities propagate and how they interact. For definiteness, we call these discontinuities waves.

2.1. **Planar waves and Rankine–Hugoniot condition.** Since system (2.1) is linear, there are no nonlinear rarefaction waves or shocks but only linear waves in solutions. As a first step we just consider a planar wave. We assume such a wave emitted from an initial discontinuity at the line $\mu x + \nu y = 0$ in the direction (μ, ν) with $\mu^2 + \nu^2 = 1$. The solution takes the form

$$(\phi, u, v)(t, x, y) = (\phi, u, v)((\mu x + \nu y)/t). \tag{2.3}$$

Let $[\phi]$ be the jump of ϕ across this discontinuity, and analogously for u and v, and $(-\sigma, \mu, \nu)$ the normal of the discontinuity. Then we get the Rankine–Hugoniot condition,

$$\begin{cases} \sigma = \sigma_0 = 0, \\ \mu[u] + \nu[v] = 0, \\ [\phi] = 0, \end{cases} \quad \text{or} \quad \begin{cases} \sigma = \sigma_\pm = \pm c, \\ [\phi] \mp (\mu[u] + \nu[v]) = 0, \\ -\nu[u] + \mu[v] = 0. \end{cases} \tag{2.4}$$

There are three possibilities for planar waves to travel with velocities 0, $\pm c$. Note that choosing an initial data with a jump along $\mu x + \nu y = 0$ leads to a solution with at most three such planar wave parts. The first system of (2.4) means that the normal components of velocity of (u, v) are identical on both sides of stationary discontinuity with $\sigma_0 = 0$. The second system means that the tangential components of velocity are identical on both sides of the discontinuities moving with speeds $\sigma_\pm = \pm c$. In this sense the case $\sigma_0 = 0$ resembles a contact discontinuity, i.e. a slip layer, and the case $\sigma_\pm = \pm c$ are something like shock waves in gas dynamics. Thus for given two initial states separated by the straight line $\mu x + \nu y = 0$, the solution can be constructed via the characteristic analysis method in the phase plane, similar to the construction of Riemann solutions for adiabatic gas dynamics, see, e.g., [3], [27]. Specifically, we solve this problem in the $(\mu u + \nu v, \phi)$–plane. Denote by $U = -\nu u + \mu v$ and $V = \mu u + \nu v$ the tangential and normal velocity components, respectively, along the plane $\mu x + \nu y = \sigma t$ with $\sigma = \sigma_0$, or $\sigma_\pm$. Then

(2.4) is equivalent to

$$V_{1*} - V_{2*} = 0 \quad \text{and} \quad \begin{array}{l} \phi_1 - \phi_* + (V_1 - V_{1*}) = 0, \\ U_1 - U_{*1} = 0, \quad U_2 - U_{2*} = 0, \\ \phi_2 - \phi_* - (V_2 - V_{2*}) = 0. \end{array} \tag{2.5}$$

Taking the initial data (2.2) to be two constant states as

$$(\phi, u, v)(t = 0, x, y) = \begin{cases} (\phi_1, u_1, v_1), & \mu x + \nu y < 0, \\ (\phi_2, u_2, v_2), & \mu x + \nu y > 0, \end{cases} \tag{2.6}$$

the solution can be expressed explicitly as

$$(\phi, u, v)(t, x, y) = \begin{cases} (\phi_1, u_1, v_1), & \mu x + \nu y < \sigma_- t, \\ (\phi_*, u_{*1}, v_{*1}), & \sigma_- t < \mu x + \nu y < 0, \\ (\phi_*, u_{*2}, v_{*2}), & 0 < \mu x + \nu y < \sigma_+ t, \\ (\phi_2, u_2, v_2), & \mu x + \nu y > \sigma_+ t. \end{cases} \tag{2.7}$$

where (ϕ_*, u_{*1}, v_{*1}) and (ϕ_*, u_{*2}, v_{*2}) are solved by using (2.5). We illustrate the construction of solutions in Figure 1.

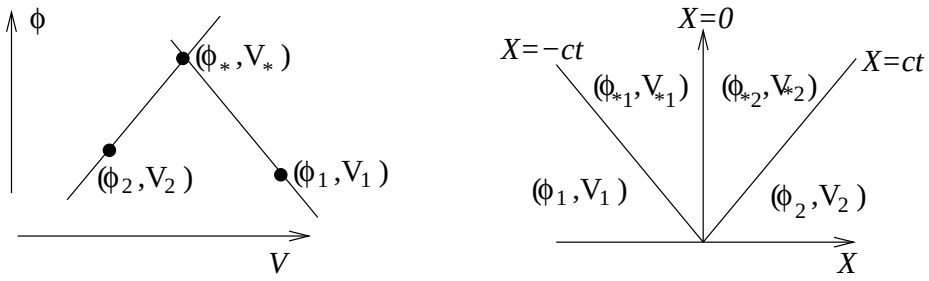

FIGURE 1. Ilustration of the construction of 2-D Riemann solutions; $X = \mu x + \nu y$, $V = \mu u + \nu v$.

In general, the initial data are constant in angular domains and the corresponding solutions will be much more complicated. However the invariance of (2.1) and (2.2) under the dilation $(t, x, y) \to (\alpha t, \alpha x, \alpha y)$ $(\alpha > 0)$ enables us to seek self–similar solutions of the form $(\phi, u, v)(t, x, y) = (\phi, u, v)(\xi, \eta)$ with $\xi = x/t, \eta = y/t$. Then under this self–similar transformation system (2.1) becomes

$$\begin{cases} -\xi\phi_\xi - \eta\phi_\eta + c(u_\xi + v_\eta) = 0, \\ -\xi u_\xi - \eta u_\eta + c\phi_\xi = 0, \\ -\xi v_\xi - \eta v_\eta + c\phi_\eta = 0 \end{cases} \tag{2.8}$$

and initial data (2.2) are transformed into boundary values at infinity

$$\lim_{\xi^2+\eta^2 \to \infty} (\phi, u, v) = (\phi_0, u_0, v_0)(\theta), \tag{2.9}$$

where $\eta/\xi = \arctan\theta$ is kept constant taking the limit. This is a boundary value problem for the first order system of partial differential equations (2.8) with boundary values (2.9) at infinity. To solve it, the concepts of characteristics and discontinuities in (ξ,η)–plane play an essential role. The eigenvalues of the system are

$$\lambda_0 = \frac{\eta}{\xi}, \quad \text{and} \quad \lambda_\pm = \frac{\xi\eta \pm c\sqrt{\xi^2+\eta^2-c^2}}{\xi^2-c^2}. \tag{2.10}$$

The eigenvalue λ_0 is always real while $\lambda_\pm$ are complex inside the **sonic circle** $S : \xi^2+\eta^2 = c^2$ and real outside this circle. In other words, the flow is subsonic inside the circle and supersonic outside the circle but parabolic degenerate on the sonic circle.

In the supersonic domain, we define characteristics,

$$\Gamma_i : \frac{d\eta}{d\xi} = \lambda_i, \quad i = 0,+,-. \tag{2.11}$$

Then it can readily be checked that Γ_0 passes through the origin, Γ_- and Γ_+ are straight and always tangent to the circle $\xi^2+\eta^2 = c^2$. Furthermore one can check that Γ_+ is tangent to S in the clockwise direction while Γ_- is tangent to S in the counterclockwise direction.

The discontinuity $\eta = \eta(\xi)$, being a discontinuity surface $y = ty(x/t)$ with the normal $(\eta-\xi\sigma,\sigma,-1)$ and $\sigma = \eta'(\xi)$ in (t,x,y)–space, satisfies the Rankine–Hugoniot condition expressed in the selfsimilar variables [15],

$$\begin{cases} \sigma_0 = \dfrac{\eta}{\xi}, \\ \sigma[u]-[v] = 0, \\ [\phi] = 0, \end{cases} \quad \text{or} \quad \begin{cases} \sigma_\pm = \dfrac{\xi\eta \pm c\sqrt{\xi^2+\eta^2-c^2}}{\xi^2-c^2}, \\ \sigma_\pm[v]+[u] = 0, \\ c\sigma_\pm[\phi]+(\eta-\xi\sigma_\pm)[u] = 0. \end{cases} \tag{2.12}$$

The discontinuities $\eta = \eta(\xi)$ defined by $\dfrac{d\eta}{d\xi} = \sigma_i$ $(i = 0,+,-)$ have the same properties as those of Γ_i. The components of velocity also share the same behaviour as those in the case of planar waves above.

For the Riemann problem under consideration, (2.1) and (2.2) are equivalent to (2.8) and (2.9). To solve the latter, we first need to solve this boundary value problem at infinity, which is due to the following lemma.

Lemma 2.1. *If the initial data (2.2) consist of a finitely many constant states, then problem (2.8) and (2.9) is locally well-posed at infinity. The solution consists of planar waves and constant states.*

The proof of this lemma is similar to that in [5]. We omit the details.

After getting the solution at infinity, we have to extend this solution inwards from an infinity. The solution can be extended by the method of characteristics until an interaction of waves occurs.

2.2. **The interaction of waves.** As preparation of the construction of global solution, the interaction of waves is now studied. We wish to solve a Riemann problem in an angular domain Θ bounded by two characteristics in the (ξ,η)–plane, which originate in a point P, where a wave interaction occurs, as illustrated in Figure 2.

Let Γ_- and Γ_+ be two discontinuities, which intersect at P, Γ_+ separates the state (ϕ_1,u_1,v_1) from (ϕ_0,u_0,v_0) and Γ_- separates (ϕ_2,u_2,v_2) from (ϕ_0,u_0,v_0).

Thus our problem is to solve (2.8) inside the domain Θ bounded by PP_1 and PP_2 with the boundary values

$$(\phi, u, v)|_{PP_1} = (\phi_1, u_1, v_1) \quad \text{and} \quad (\phi, u, v)|_{PP_2} = (\phi_2, u_2, v_2). \tag{2.13}$$

This is a Goursat-type problem with a possibly discontinuous boundary value on the characteristics. Note that if $(\phi_1, u_1, v_1) \neq (\phi_2, u_2, v_2)$, the solution cannot be expected to be continuous. Therefore we attempt to seek discontinuous solutions. Denote $P = (\xi_0, \eta_0)$, and consider a solution of the form

$$(\phi, u, v) = (\phi, u, v)(\zeta), \quad \zeta = \zeta(\xi, \eta) = \frac{\eta - \eta_0}{\xi - \xi_0}. \tag{2.14}$$

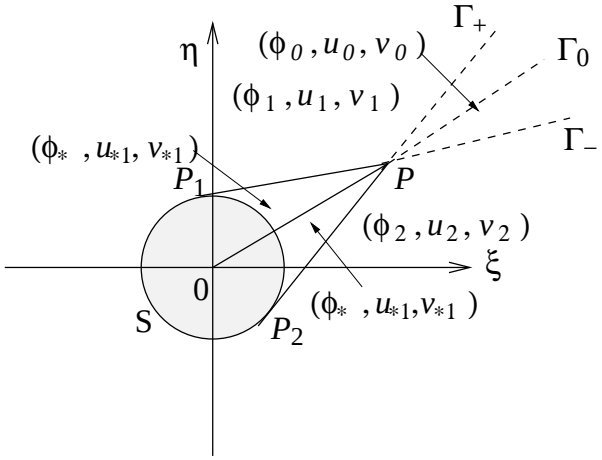

FIGURE 2. The Riemann problem in an angular domain; the discontinuities Γ_j have the respective slopes σ_j $j = 0, -, +$; $S : \xi^2 + \eta^2 = c^2$.

The curve $\zeta = \zeta(\xi, \eta)$ is actually a surface $y = t(\zeta(x/t - \xi_0) + \eta_0)$ with the normal $(\eta_0 - \zeta\xi_0, \zeta, -1)$ in (t, x, y)–space. Therefore, the Rankine–Hugoniot condition of discontinuities of this form satisfy (2.12) just replacing $(\eta - \sigma\xi, \sigma, -1)$ by $(\eta_0 - \zeta\xi_0, \zeta, -1)$.

The slopes of the straight lines PP_2, PP_1 and PO are exactly ζ_+, ζ_- and ζ_0. $\zeta_\pm$ must be real as long as (ξ_0, η_0) is located in the supersonic domain. This shows that the solution of the form (2.14) can always be sought if two waves interact in the supersonic domain.

If $(\phi_1, u_1, v_1) = (\phi_2, u_2, v_2)$, then the solution in Θ is just constant. Otherwise, let PP_i separate (ϕ_i, u_i, v_i) from (ϕ_*, u_{*i}, v_{*i}), $i = 1, 2$, and PO separate (ϕ_*, u_{*1}, v_{*1}) and (ϕ_*, u_{*2}, v_{*2}). Then we have the following relations by using the Rankine–Hugoniot condition (2.12):

Across PP_1,

$$\begin{cases} \zeta_-(v_1 - v_{*1}) + (u_1 - u_{*1}) = 0, \\ a(u_1 - u_{*1}) - c\zeta_-(\phi_1 - \phi_*) = 0, \quad a = -\eta_0 + \zeta_-\xi_0; \end{cases} \tag{2.15}$$

across PP_2,

$$\begin{cases} \zeta_+(v_2 - v_{*2}) + (u_2 - u_{*2}) = 0, \\ b(u_2 - u_{*2}) - c\zeta_+(\phi_2 - \phi_*) = 0, \quad b = -\eta_0 + \zeta_+\xi_0; \end{cases} \tag{2.16}$$

and across PO,

$$-\zeta_0(u_{*1}-u_{*2})+(v_{*1}-v_{*2})=0. \tag{2.17}$$

We write the system of equations (2.15)–(2.17) as

$$\underline{\underline{A}}\,\underline{U}_*=\underline{B}, \tag{2.18}$$

where

$$\underline{\underline{A}}=\begin{pmatrix} -1 & 0 & -\zeta_- & 0 & 0\\ -a & 0 & 0 & 0 & c\zeta_-\\ 0 & -1 & 0 & -\zeta_+ & 0\\ 0 & -b & 0 & 0 & c\zeta_+\\ -\zeta_0 & \zeta_0 & 1 & -1 & 0 \end{pmatrix},\ \underline{U}_*=\begin{pmatrix} u_{*1}\\ u_{*2}\\ v_{*1}\\ v_{*2}\\ \phi_* \end{pmatrix},\ \underline{B}=\begin{pmatrix} -\zeta_- v_1-u_1\\ -au_1+\zeta_- c\phi_1\\ -\zeta_+ v_2-u_2\\ -bu_2+\zeta_+ c\phi_2\\ 0 \end{pmatrix}. \tag{2.19}$$

Note that

$$\det\underline{\underline{A}}=c\zeta_-\zeta_+(\zeta_+-\zeta_-)(\xi_0+\eta_0\zeta_0)\neq 0 \tag{2.20}$$

if $\zeta_-\zeta_+\neq 0$ and by (2.12) $\zeta_+\neq\zeta_-$, i.e. (ξ_0,η_0) is not located on the circle $\xi^2+\eta^2=c^2$. If $\zeta_-\zeta_+=0$, then $\xi_0=\pm c$ or $\eta_0=\pm c$. Without loss of generality, we just consider the case $\xi_0=c$. Then (2.16) is replaced by

$$\begin{cases} v_2-v_{*2}=0,\\ u_2-u_{*2}-c(\phi-\phi_*)=0 \end{cases} \tag{2.21}$$

and $\zeta_-=\dfrac{\eta_0^2-c^2}{2c\eta_0}$. In all, the system (2.15), (2.17), (2.21) has a unique solution when P is located outside the sonic circle. Thus the Goursat-type problem (2.8) and (2.13) is uniquely solvable with the structure sketched in Figure 2.

2.3. **The subsonic problem.** In order to get the global Riemann solutions, we have to study the subsonic problem (2.8) inside the sonic domain with the boundary value on the sonic circle resulting from the extension of the Riemann solution in the supersonic domain. The sonic circle is a degenerate boundary. The boundary values are piecewise constant. For simplicity, denote the subsonic domain by $\Omega=\{(\xi,\eta);\xi^2+\eta^2<c^2\}$.

System (2.8) can be rewritten in the operator form

$$\underline{\underline{L}}(\underline{w})=(L_1(\underline{w}),L_2(\underline{w}),L_3(\underline{w}))^{\mathrm{T}}:=\underline{\underline{A}}_1\underline{w}_\psi+\underline{\underline{A}}_2\underline{w}_\eta=0,\qquad \underline{w}=(\phi,u,v)^{\mathrm{T}}, \tag{2.22}$$

where

$$\underline{\underline{A}}_1:=\begin{pmatrix} -\xi & c & 0\\ c & -\xi & 0\\ 0 & 0 & -\xi \end{pmatrix},\quad \underline{\underline{A}}_2:=\begin{pmatrix} -\eta & 0 & c\\ 0 & -\eta & 0\\ c & 0 & -\eta \end{pmatrix}.$$

Correspondingly, the adjoint operator of $\underline{\underline{L}}$ is denoted by $\underline{\underline{L}}^*=(L_1^*,L_2^*,L_3^*)^{\mathrm{T}}$, i.e.

$$\underline{\underline{L}}^*(\underline{\alpha})=\begin{pmatrix} (\xi\alpha_1)_\xi+(\eta\alpha_1)_\eta & -c\alpha_{1\xi} & -c\alpha_{1\eta}\\ -c\alpha_{2\xi} & (\xi\alpha_2)_\xi+(\eta\alpha_2)_\eta & 0\\ -c\alpha_{3\eta} & 0 & (\xi\alpha_3)_\xi+(\eta\alpha_3)_\eta \end{pmatrix}, \tag{2.23}$$

where $\underline{\alpha}=(\alpha_1,\alpha_2,\alpha_3)$, the subscripts "$\xi$" and "$\eta$" represent the partial derivatives as before.

According to Friedrichs [8] a first order system of type (2.22) is a **symmetric positive system**. Due to regularity of the boundary $\partial\Omega$ we have everywhere the outer normal vector field $\underline{n}=(n_1,n_2)$ and can define the boundary operator

$$\underline{\underline{B}}\ :=\ \underline{\underline{A}}_1n_1+\underline{\underline{A}}_2n_2.$$

Thus,

$$\underline{\underline{B}} = \begin{pmatrix} -\xi n_1 - \eta n_2 & cn_1 & cn_2 \\ cn_1 & -\xi n_1 - \eta n_2 & 0 \\ cn_2 & 0 & -\xi n_1 - \eta n_2 \end{pmatrix}.$$

Now we take $\underline{\underline{B}}^-$ to be the negative part of the symmetric matrix $\underline{\underline{B}}$, i.e. $\underline{\underline{B}}^-$ is negative semi-definite and $\underline{\underline{B}}^+ = \underline{\underline{B}} - \underline{\underline{B}}^-$ is positive semi-definite. Let $\underline{g} \in L^2(\partial\Omega)$ be given. Then according to Friedrichs [8], see also Lax and Phillips [13], an admissible boundary condition is defined via

$$\underline{\underline{B}}^- \underline{w} \;=\; \underline{\underline{B}}^- \underline{g} \quad \text{on} \quad \partial\Omega. \tag{2.24}$$

A weak solution of (2.22) and (2.24) can be defined as follows.

Definition 2.1. Let $\underline{g}$ be in $L^2(\partial\Omega)$. A measurable vector $\underline{w} = (\phi, u, v) \in L^2(\Omega)$ is a weak solution of (2.22) and (2.24) iff

$$(\underline{w}, \underline{\underline{L}}^* \underline{\alpha}) + \langle \underline{\underline{B}}^- \underline{g}, \underline{\alpha} \rangle_{\partial\Omega} = 0, \tag{2.25}$$

for all $\underline{\alpha} \in C^1(\Omega) \cap C(\bar{\Omega})$.

The following theorem is due to Friedrichs [8], see also Lax and Phillips [13], and gives the existence and uniqueness of solution in the strong sense.

Theorem 2.2. *Let $\underline{g} \in L^2(\partial\Omega)$. Then the problem (2.22), (2.24) has a unique solution $\underline{w} = (\phi, u, v) \in L^2(\Omega)$, s.t.*

$$\underline{\underline{L}}\,\underline{w} = 0 \qquad \textit{a. e. on } \Omega$$

$$\underline{\underline{B}}^- \underline{w} = \underline{\underline{B}}^- \underline{g} \qquad \textit{on } \partial\Omega.$$

Note that ϕ satisfies in a weak sense the following differential equations of second order, which can be derived from (2.8) for smooth as well as distributional solutions

$$Q(\phi) = (c^2 - \xi^2)\phi_{\xi\xi} - 2\xi\eta\phi_{\xi\eta} + (c^2 - \eta^2)\phi_{\eta\eta} - 2(\xi\phi_\xi + \eta\phi_\eta) = 0. \tag{2.26}$$

If this equation has a unique classical solution, then the solution satisfies the maximum principle.

Lemma 2.3. (MAXIMUM PRINCIPLE) *Suppose the solution of (2.26) satisfies $\phi \in C^2(\Omega) \cap C(\bar{\Omega})$. Then the maximum principle holds, i.e.*

$$\|\phi\|_{L^p(\Omega)} \le \left(\frac{c}{2}\right)^{1/p} \|\phi\|_{L^p(\partial\Omega)} \tag{2.27}$$

for all $1 \le p < \infty$. For $p = \infty$, it is

$$\max_{\Omega} |\phi| \le \max_{\partial\Omega} |\phi|. \tag{2.28}$$

Proof. The adjoint operator to Q is

$$Q^*(\beta) = ((c^2 - \xi^2)\beta)_{\xi\xi} - (2\xi\eta\beta)_{\xi\eta} + ((c^2 - \eta^2)\beta)_{\eta\eta} + 2\xi\beta_\xi + 2\eta\beta_\eta + 4\beta.$$

Applying Green's formula, we have

$$\int_\Omega w Q^*(\beta) d\xi d\eta - \int_\Omega \beta Q(w) d\xi d\eta = -c \int_{\partial\Omega} w\beta d\sigma$$

for $w, \beta \in C^2(\Omega) \cap C(\bar{\Omega})$. Taking $\beta = -1$ and $w = (\phi^2 + \delta)^{p/2}$ for some $\delta > 0$, we have $Q^*(\beta) = 2$ and

$$\begin{aligned} Q(w) = \quad & p(\phi^2+\delta)^{p/2-1}\phi Q(\phi) \\ & +p(\phi^2+\delta)^{p/2-2}\left((p-1)\phi^2+\delta\right)((c^2-\xi^2)\phi_\xi^2 - 2\xi\eta\phi_\xi\phi_\eta + (c^2-\eta^2)\phi_\eta^2). \end{aligned}$$

Since $(c^2-\xi^2)\phi_\xi^2 - 2\xi\eta\phi_\xi\phi_\eta + (c^2-\eta^2)\phi_\eta^2 \geq 0$ and $Q(\phi) = 0$, we get

$$2\int_\Omega (\phi^2+\delta)^{p/2} \leq c\int_{\partial\Omega} (\phi^2+\delta)^{p/2} d\sigma.$$

Letting $\delta \to 0$, we arrived at (2.27). The formula (2.28) is obvious from (2.27). □

The general boundary value problem for (2.26) is also well–posed. This is very similar to Theorem 1.5.1 in [24]. We state this theorem in the following theorem.

Theorem 2.4. *There exists a unique solution of (2.26) with a measurable boundary value $\phi|_{\partial\Omega} = \bar{\phi}$ in the sense that*

$$\int_\Omega Q^*(\beta)\phi d\xi d\eta = -c\int_{\partial\Omega} \bar{\phi}\beta d\sigma \tag{2.29}$$

for all $\beta \in C^2(\Omega) \cap C(\bar{\Omega})$. This solution satisfies the maximum principle

$$|\phi| \leq \max_{\partial\Omega} |\bar{\phi}|. \tag{2.30}$$

The proof of this theorem basically follows that of Theorem 1.5.1 in [24]. We omit the details.

2.4. **The construction of global Riemann solutions.** Based on the above preparation, we can solve the two dimensional Riemann problem (2.1) for a finitely many constant states in the initial data (2.2). By Lemma 2.2, we conclude that the solution at infinity consists of piecewise constant states separated by planar waves. These waves can be continued up to the sonic circle. In view of the Rankine-Hugoniot conditions (2.15) - (2.17), these waves cannot be curved at interaction points, where the Goursat-type problem can be solved, as explained in Subsection 2.2. Thus we can completely solve (2.8) and (2.9) outside of subsonic domain using the method of characteristics. By Theorems 2.1 and 2.2 we obtain the combination of the solution inside the subsonic domain. Thus a unique global Riemann solution is constructed. Similar construction of solutions for gas dynamics can be found in [15].

3. **Evolution Galerkin methods.** The evolution Galerkin methods (EG) were proposed by Lukáčová, Morton and Warnecke in [17] as numerical schemes for solving multidimensional systems of hyperbolic conservation laws. The main idea of the evolution Galerkin methods is that they evolve the initial data using the bicharacteristic cone or the Mach cone and then project them onto a finite element space. In [17] three new first order evolution Galerkin schemes (EG1-EG3) for a system of hyperbolic equations, and particularly for the wave equation system were derived and analyzed. It has been shown in [17], see also [22], that the EG methods capture very well such solution properties as circular symmetry, independence of mesh orientation, vorticity preservation and shocks. The accuracy of some of these first order schemes, e.g. the EG3 scheme, matches on coarse meshes that of the commonly used second order schemes, e.g. the Lax-Wendroff.

In [17] we proved that the EG schemes are stable upto some CFL number $0 < \nu_{\max} < 1$ and numerical tests, presented in [19], indicate the bounds of $\nu_{\max}$ for each approximate evolution operator EG1 - EG3.

In order to derive higher order versions of the EG schemes a finite volume formulation is used. Thus to compute fluxes on the cell interfaces the approximate solution is evolved using one of the three approximate evolution operators mentioned above. Then using a suitable recovery operator and a numerical quadrature for time integral we obtain high resolution finite volume evolution Galerkin schemes, see [16], [18], [20], [19].

Let us note here that the commonly used finite volume methods approximate fluxes on the cell interfaces by solving a Riemann problem in normal directions to the cell interfaces. However, it has been shown by many authors, see e.g. [6], [7], [14], [17], [23], that such an approach can lead to structural deficiencies in the numerical solution. Our finite volume evolution Galerkin methods take advantages of both approaches: the simplicity of the finite volume formulation and the multidimensionality of the evolution Galerkin schemes. In fact, they combine the usually conflicting design objectives of using the conservation form and following the characteristics, or bicharacteristics. This is a novel feature of our method and a genuine multidimensional generalization for systems of Godunov's idea.

In what follows we will describe explicitly evolution Galerkin schemes, finite volume evolution Galerkin schemes and their higher order version. The wave equation system (2.1) can be written in the form of a general system of hyperbolic conservation laws in d space dimensions

$$\underline{U}_t + \sum_{k=1}^{d} \left(\underline{F}_k(\underline{U})\right)_{x_k} = 0, \;\; \underline{x} = (x_1, \ldots, x_d)^T \in I\!R^d, \tag{3.1}$$

where $\underline{F}_k = \underline{F}_k(\underline{U}), k = 1, \ldots, d$ represent given physical flux functions and the conservative variables are $\underline{U} = (u_1, \ldots, u_m)^T \in I\!R^m$. Let us denote by $E(s) : [H^k(I\!R^d)]^m \to [H^k(I\!R^d)]^m$ the exact evolution operator associated with a time step s acting on Sobolev spaces for the system (3.1), i.e.

$$\underline{U}(\cdot, t+s) = E(s)\underline{U}(\cdot, t). \tag{3.2}$$

We suppose that S_h^p is a finite element space consisting of piecewise polynomials of order $p \geq 0$. Let $\underline{U}^n$ be an approximation in the space S_h^p to the exact solution $\underline{U}(\cdot, t_n)$ at a time $t_n > 0$ and take $E_\tau : S_h^r \to [H^k(I\!R^d)]^m$ to be a suitable approximation to the exact evolution operator $E(\tau)$, $r \geq 0$. We denote by $P_h : [H^k(I\!R^d)]^m \to S_h^p$ an L^2-projection onto cells, and by $R_h : S_h^p \to S_h^r$ a recovery operator, $r \geq p \geq 0$. We limit our considerations to cases of constant time step Δt, i.e. $t_n = n\Delta t$, and of a uniform mesh consisting of d-dimensional cubes with a uniform mesh size h.

Definition 3.1 (EG methods)**.** *Starting from some initial value $\underline{U}^0$ at time $t = 0$, the higher order evolution Galerkin scheme (EG) falls into the class of PERU-schemes and is recursively defined by means of*

$$\underline{U}^{n+1} = P_h E_\Delta R_h \underline{U}^n.$$

Definition 3.2 (FVEG methods)**.** *The recursive update formula for the finite volume evolution Galerkin method (FVEG) reads*

$$\underline{U}^{n+1} = \underline{U}^n - \frac{1}{h}\int_0^{\Delta t}\sum_{k=1}^{d}\delta_{x_k}\underline{F}_k(\underline{U}^{n+\tau/\Delta t})\,d\tau, \tag{3.3}$$

where the spatial central difference $v(x+h/2)-v(x-h/2)$ is denoted by $\delta_x v(x)$ and $\delta_{x_k}\underline{F}_k(\underline{U}^{n+\tau/\Delta t})$ represents an approximation to the edge flux difference at intermediate time levels $t_n+\tau$, $\tau\in]0,\Delta t[$. The cell boundary flux $F_k\left(\underline{U}^{n+\tau/\Delta t}\right)$ is evolved using the approximate evolution operator E_τ to $t_n+\tau$ and averaged along the cell boundary, i.e. e.g. on vertical edge for $\underline{U}$ itself

$$\underline{U}^{n+\tau/\Delta t} = \frac{1}{h}\int_0^h E_\tau R_h \underline{U}^n\,dS_y\,d\tau. \tag{3.4}$$

An analogous formula holds for the horizontal edges.

Now we will give the approximate evolution operators E_Δ for the wave equations system (2.1) that we have used.

3.1. **Approximate evolution operators.** Consider the Mach cone corresponding to the wave equation system (2.1), see Figure 3. Let us denote by $P=(x,y,t+\Delta t)$ the apex of the Mach cone and by $Q=Q(\theta)=(x+c\Delta t\cos\theta, y+c\Delta t\sin\theta, t)$ the base points parametrized by the angle $\theta\in[0,2\pi]$. Denote by $P'=(x,y,t)$ the center of the base of the cone. The lines from $Q(\theta)$ to P generating the mantle of the so-called bicharacteristic cone as well as the center line are called bicharacteristics.

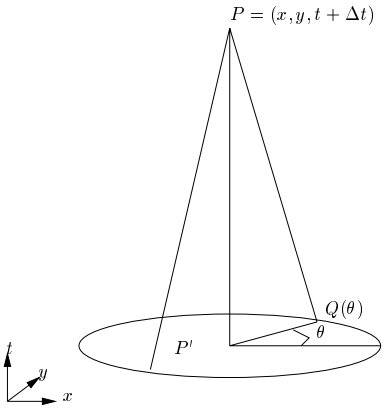

FIGURE 3. Bicharacteristics along the Mach cone through P and $Q(\underline{\theta})$ as well as P'.

Using the theory of bicharacteristics it can be shown that the solution (ϕ, u, v) at the point P is determined by its values on the base as well as on the mantle of the characteristic cone. An exact integral equation has been derived; for details see e.g. [1], [25], [17]. It should be pointed out that this integral equation is not an integral representation of the solution in terms of the data, such as the Kirchhoff formula for the wave equation. Different discretizations with respect to time of this integral equation lead to the following approximate evolution operators E_Δ. For more details on their construction see [17], [22].

3.2. **Approximate evolution operator for the EG1 scheme.**

$$\phi_P = \frac{1}{2\pi}\int_0^{2\pi} \phi_Q - 2u_Q\cos\theta - 2v_Q\sin\theta \mathrm{d}\theta + O(\Delta t^2) \tag{3.5}$$

$$u_P = \frac{1}{\pi}\int_0^{2\pi} -\phi_Q\cos\theta + u_Q(3\cos^2\theta - 1) + 3v_Q\sin\theta\cos\theta \mathrm{d}\theta + O(\Delta t^2) \tag{3.6}$$

$$v_P = \frac{1}{\pi}\int_0^{2\pi} -\phi_Q\sin\theta + 3u_Q\sin\theta\cos\theta + v_Q(3\sin^2\theta - 1)\mathrm{d}\theta + O(\Delta t^2) \tag{3.7}$$

3.3. **Approximate evolution operator for the EG2 scheme.**

$$\phi_P = \frac{1}{\pi}\int_0^{2\pi} \phi_Q - u_Q\cos\theta - v_Q\sin\theta \mathrm{d}\theta - \phi_{P'} + O(\Delta t^3) \tag{3.8}$$

$$u_P = \frac{1}{\pi}\int_0^{2\pi} -\phi_Q\cos\theta + u_Q(2\cos^2\theta - \tfrac{1}{2}) + 2v_Q\sin\theta\cos\theta \mathrm{d}\theta + O(\Delta t^3) \tag{3.9}$$

$$v_P = \frac{1}{\pi}\int_0^{2\pi} -\phi_Q\sin\theta + 2u_Q\sin\theta\cos\theta + v_Q(2\sin^2\theta - \tfrac{1}{2})\mathrm{d}\theta + O(\Delta t^3) \tag{3.10}$$

3.4. **Approximate evolution operator for the EG3 scheme.**

$$\phi_P = \frac{1}{2\pi}\int_0^{2\pi} \phi_Q - 2u_Q\cos\theta - 2v_Q\sin\theta \mathrm{d}\theta + O(\Delta t^2) \tag{3.11}$$

$$u_P = \frac{1}{2}u_{P'} + \frac{1}{2\pi}\int_0^{2\pi} -2\phi_Q\cos\theta + u_Q(3\cos^2\theta - 1) + 3v_Q\sin\theta\cos\theta \mathrm{d}\theta + O(\Delta t^2) \tag{3.12}$$

$$v_P = \frac{1}{2}v_{P'} + \frac{1}{2\pi}\int_0^{2\pi} -2\phi_Q\sin\theta + 3u_Q\sin\theta\cos\theta + v_Q(3\sin^2\theta - 1)\mathrm{d}\theta + O(\Delta t^2) \tag{3.13}$$

Denote by P_h an L^2 - projection onto a space of piecewise constant functions S_h^0 and apply P_h to the approximate evolution operators (3.5)-(3.7), (3.8)-(3.10), (3.11)-(3.13). This yields the first order schemes $\underline{U}^{n+1} = P_h E_\Delta \underline{U}^n$, which in [17] are referred to as the EG1, EG2 and EG3 schemes. Space integrals coming from the projection step are computed exactly, i.e. no numerical quadrature is used. The resulting finite difference formulation on equidistant rectangular meshes can be found in [17], where the coefficients of the EG schemes in finite difference formulation are given explicitly.

3.5. **Second order finite volume evolution Galerkin schemes.** There are many possible recovery schemes, which could be used. We only prescribe that the following **conservativity property** holds

$$P_h R_h \underline{V} = \underline{V} \qquad \text{for all } \underline{V} \in S_h^p. \tag{3.14}$$

For our computations we choose a discontinuous bilinear recovery using a finite difference approximation to derivatives, but others could be used and were tested as well. The formula for the recovery on each cell is

$$\begin{aligned} R_h \underline{U}|_{\varnothing_{ij}} = \underline{U}_{ij} &+ \frac{(x-x_i)}{4h}\left(\Delta_{0x}\underline{U}_{ij+1} + 2\Delta_{0x}\underline{U}_{ij} + \Delta_{0x}\underline{U}_{ij-1}\right) \\ &+ \frac{(y-y_j)}{4h}\left(\Delta_{0y}\underline{U}_{i+1j} + 2\Delta_{0y}\underline{U}_{ij} + \Delta_{0y}\underline{U}_{i-1j}\right) \\ &+ \frac{(x-x_i)(y-y_j)}{h^2}\Delta_{0y}\Delta_{0x}\underline{U}_{ij}, \end{aligned}$$

where $\Delta_{0x} v(x) = \frac{1}{2}\left[v(x+h) - v(x-h)\right] = \frac{1}{2}\left(v_{i+1} - v_{i-1}\right)$, an analogous notation is used for Δ_{0y}.

For the computation of fluxes through cell edges the cell interface value of $\underline{U}$ has to be determined. Instead of the exact time integration the second order midpoint rule is used. Thus, the finite volume evolution Galerkin scheme (3.3) now is written as

$$\underline{U}^{n+1} = \underline{U}^n - \frac{\Delta t}{h}\sum_{k=1}^{d} \delta_{x_k} \underline{F}_k(\underline{U}^{n+*}), \tag{3.15}$$

where

$$\underline{F}_k(\underline{U}^{n+*}) = \frac{1}{h}\int_0^h F_k(E_{\Delta t/2} R_h \underline{U}^n)\mathrm{d}S. \tag{3.16}$$

The resulting two-dimensional space integrals of the bilinear function $R_h \underline{U}^n$ with respect to θ and cell edges are computed exactly without any numerical quadrature and thus all of the infinitely many directions of propagation of flow information are taken explicitly into account. Examples of stencils can be found in [18]. The above construction leads for every approximate evolution operator (3.5)-(3.7), (3.8)-(3.10), (3.11)-(3.13) to an overall second order scheme. Numerical experiments show, see [16], [18], that these schemes give very accurate results in regions were the solution is smooth, e.g. even 7 times more accurate than the commonly used second order schemes of Lax-Wendroff and finite volume flux vector splitting scheme using the MUSCL approach. In what follows we will test the quality of the numerical solution for a discontinous genuinely multidimensional test case.

4. **Numerical results.** The goal of this section is to solve numerically a two-dimensional Riemann problem with the initial data consisting of finitely many constant states. Using the results from the Section 2 the exact analytical solution outside the subsonic region can be found. The exact solution will be compared with the numerical solution obtained by the evolution Galerkin schemes as well as by other commonly used numerical schemes. Thus, we will get a good insight into the performance of our schemes and the possibility to compare the numerical solutions with the exact discontinuous solution, which in certain cases are available.

In what follows, let us consider the following Riemann problem

$$\begin{aligned} &\phi(\underline{x},0) = 0, \\ &v(\underline{x},0) = u(\underline{x},0) = \tfrac{1}{\sqrt{2}} \begin{cases} 1, & |y| < |x|, \\ -1, & \text{elsewhere.} \end{cases} \end{aligned} \tag{4.1}$$

The computational domain is taken to be $[-1,1] \times [-1,1]$ and the final time set to be $T = 0.4$. According to the results from the Section 2 we find out that from each of the initial discontinuities $x = \pm y$ planar waves propagate with the speeds $\sigma_0 = 0$ or $\sigma_\pm = \pm c$. For each initial discontinuity a corresponding Riemann problem has to be solved in order to find the intermediate constant states (ϕ_*, u_{*1}, v_{*1}) and (ϕ_*, u_{*2}, v_{*2}) up to the region where the waves interact, i.e. up to the points P, Q as depicted in Figure 4.

For our test case these constant states of the solution are as follows. In the regions denoted in Figure 4 by (1) - (4) $\phi = 0$; further $u = v = 1/\sqrt{2}$ in (1),(3) and $u = v = -1/\sqrt{2}$ in (2),(4). In the region between the rays l_{21} and l_{23} one has $\phi = 1$ and $u = v = 0$. Analogously, between l_{41} and l_{43} we have $\phi = -1$ and $u = v = 0$. Further, in the region between the rays l_{31} and l_{33} the values are $\phi = 0$, but $u = v = 1/\sqrt{2}$ in the region $l_{31} - l_{32}$, and $u = v = -1/\sqrt{2}$ in the region $l_{32} - l_{33}$. Similar results with opposite signs hold in the region $l_{11} - l_{13}$. Further, there are four regions corresponding to the Goursat-type problems, cf. Section 2.2. In two of them between the rays $l_{11} - l_{43}$ and $l_{33} - l_{41}$ we have $\phi = -1$ and $u = v = 0$ and analogously in the next two Goursat-type regions, which are bounded by the rays $l_{13} - l_{21}$ and $l_{23} - l_{31}$, the solution is $\phi = 1$ and $u = v = 0$.

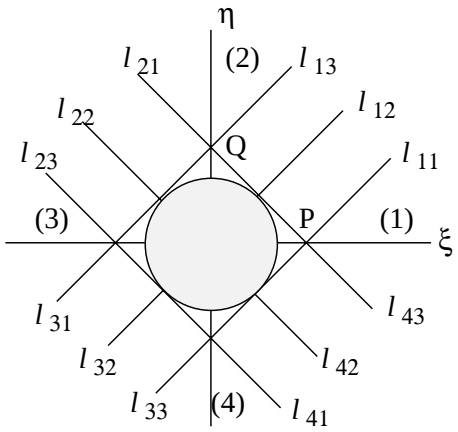

FIGURE 4. Construction of solution of the Riemann problem (4.1).

In what follows we will compare these values of the exact solution with the corresponding parts of the numerical solutions obtained by the evolution Galerkin methods as well as by other numerical schemes. We divide the computational domain into $N \times N$ mesh cells with $N = 400$. For the CFL condition $c\Delta t/h \le \nu$, we set the CFL-number $\nu = 0.55$ and take the final time $T = 0.4$.

In Figures 5 and 6 the isolines of $x-$component of velocity computed by several numerical schemes are shown. We see that two discontinuities propagate in the positive and negative direction of the diagonal $x = -y$ and an additional steady

discontinuity occurs along the main diagonal $x = y$. This is in a full agreement with the structure of the exact solution as derived above.

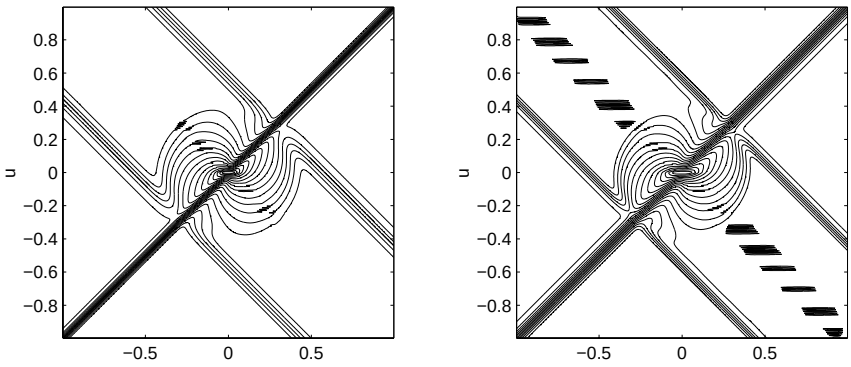

FIGURE 5. Isolines of velocity obtained by the first order FVEG3 and FV-FVS schemes.

In Figure 5 the comparison between the first order FVEG3 and the first order FV flux vector splitting (FV-FVS) method is shown. It can be seen very well that the directional splitting can spoil the structure of the solution if the discontinuity is not aligned with the mesh orientation.

Figure 6 shows the comparison of the second order FVEG3 method with the commonly known Lax-Wendroff (rotated Richtmyer) scheme. We can see that the resolution by the FVEG method is generally better without producing oscillations. Moreover comparing results of the first order and the second order FVEG3 method, Figures 5 and 6, it can be seen very well that the discontinuities are sharper and better resolved by the second order method.

Having outside the subsonic domain the analytical formulae for the exact solution, we are moreover able to compare errors between the exact and approximate

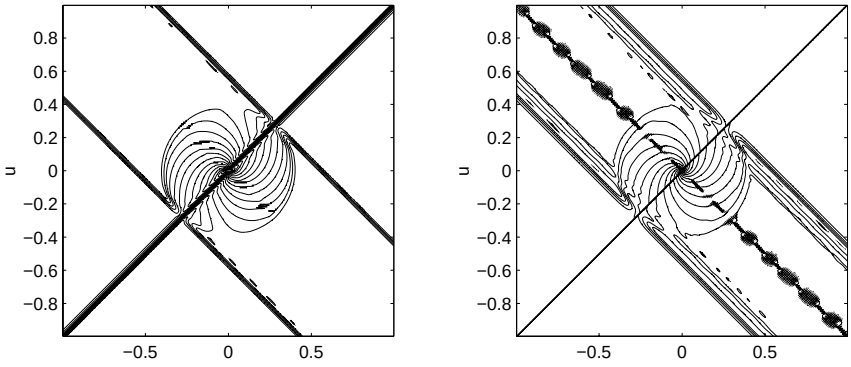

FIGURE 6. Isolines of velocity obtained by the second order FVEG3 and the Lax-Wendroff schemes.

solutions. Actually, as alreday pointed out one can use the Kirchhoff formula to obtain the exact solution in the subsonic domain also, see [10] for details. We have refrained from using it, because the accuracy at the oblique discontinuities was the main objective of our comparisons.

The CFL-number is set to 0.55, but numerical tests for several other values of CFL number and final time T confirm the behaviour of the schemes as depicted in Tables 1 and 2, where the errors between the exact and the approximate solution measured in the discrete L^2 -norm are shown. The computational domain is divided into $N \times N$ mesh cells with $N = 50, 100$.

Similarly, as we have reported in [17], [18] for the continuous data case, the EG3 scheme is the most favourable among the *first order* EG-schemes due to its lower numerical diffusion, see [21]. On the other hand, the commonly used dimensional splitting finite volume flux vector splitting scheme (FV-FVS) has not only a relatively large amount of diffusion, but can also spoil a solution considerably, see Figure 5 and Table 1.

As illustrated in Table 2 the accuracy of the *second order* FVEG1 and FVEG3 schemes is comparable with the accuracy of the second order Butler scheme [1], and it is even better than the accuracy of the Lax-Wendroff scheme. This feature has already been noticed for continuous data problems in our previous papers [16], [18], where we have shown that the accuracy of the second order FVEG schemes, namely the FVEG3 and the FVEG1, is relatively high, in comparison to other commonly used second order methods, e.g. the Lax-Wendroff scheme or the FV-FVS (MUSCL). Moreover, also the qualitative phenomena in the exact solutions are resolved better by the EG schemes as demonstrated in Figures 5 - 6. Note that although we can see some improvements in L^2-errors if the number of mesh cells increases, i.e. $N = 50, 100$, as well as if the order of method increases, we cannot actually obtain experimentally the full order of convergence in the discontinuous data case. This is a well-known fact for discontinuous data problems.

In Table 3 we show that the L^2-error computed only on the Goursat-type domain, i.e. the domain where the waves emitted from the original discontinuities start to interact. We can see the superiority of the FVEG schemes. Actually, the solution in this domain, which is close to the subsonic part, i.e. partially elliptic part, of the solution is much better and more stably approximated by the FVEG schemes than by the other second order methods that we have tested.

TABLE 1. L^2 error: comparison of first order methods outside the subsonic domain.

N	**EG1**	**EG2**	**EG3**	**FVEG3**	**FV-FVS**
50	0.659197	0.748516	0.588118	0.688988	0.710322
100	0.558413	0.640843	0.472754	0.582529	0.639134

Finally, we present in Figure 7 an example of a cross section of the ϕ component showing that for the subsonic domain the local maximum principle, derived in Section 2.3, is maintained by our schemes. We can see that the EG-schemes, the first order EG3 as well as the second order FVEG3, provide monotone solutions

TABLE 2. L^2 error: comparison of second order methods outside the subsonic domain.

N	**FVEG1**	**FVEG2**	**FVEG3**	**LW**	**Butler**
50	0.517610	0.590799	0.528176	0.565938	0.531510
100	0.404097	0.512992	0.409156	0.427599	0.408781

TABLE 3. L^2 error: comparison of second order methods in the Goursat-type domain.

N	**FVEG1**	**FVEG2**	**FVEG3**	**LW**	**Butler**
50	0.093271	0.079240	0.099798	0.127834	0.116926
100	0.060055	0.053268	0.066472	0.093554	0.081193

on the interval $[-0.4, 0.4]$, which corresponds to the subsonic domain. For the Lax-Wendroff method this is not the case.

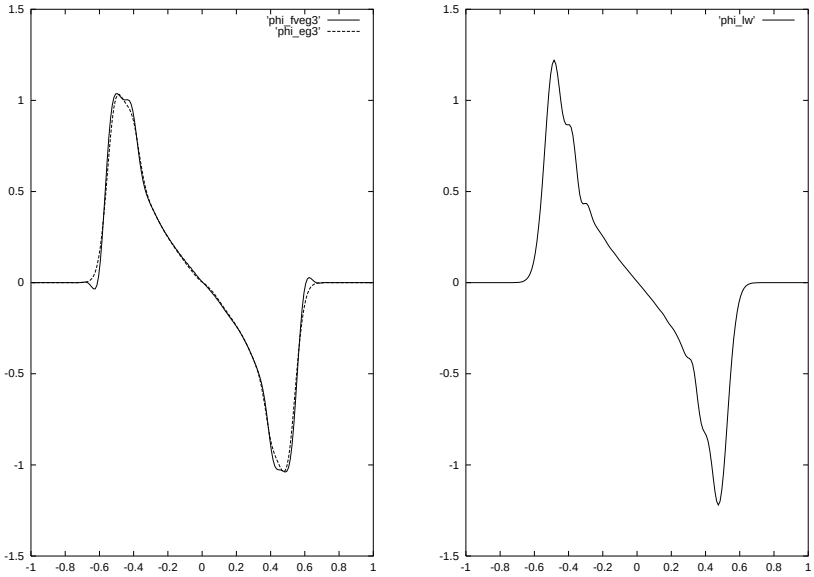

FIGURE 7. Comparison of the EG-schemes and the Lax-Wendroff method on the cross section $y = 0$, CFL=0.55, $N = 200$.

REFERENCES

[1] Butler, D.S. (1960): The numerical solution of hyperbolic systems of partial differential equations in three independent variables. *Proc. Roy. Soc.* **255A**, 233–252

[2] Brio, M.; Zakharian, A.R.; Webb, G.M. (2001): Two-dimensional Riemann solver for Euler equations of gas dynamics. *J. Comp. Phys.* **167(1)**, 177-195

[3] Chang, T.; Hsiao, L. (1989): *The Riemann problem and interaction of waves in gas dynamics.* Pitman Monographs and Surveys in Pure and Applied Mathematics 41, Longman

[4] Courant, R.; Friedrichs, K.O. (1948): *Supersonic flow and shock waves.* Interscience

[5] Čanić, S.; Keyfitz, B.L. (1998): Quasi–one–dimensional Riemann problems and their role in self–similar two dimensional flows. *Arch Rational Mech. Anal.* **144**, 233–258

[6] Fey, M. (1998): Multidimensional upwinding, Part I. The method of transport for solving the Euler equations. *J. Comp. Phys.* **143**, 159-180

[7] Fey, M. (1998): Multidimensional upwinding, Part II. Decomposition of the Euler equations into advection equations. *J. Comp. Phys.* **143**, 181-199
[8] Friedrichs, K.O. (1958): Symmetric positive linear differential equations. *Comm. Pure Appl. Math.* **XI**, 333-418
[9] Gilbarg, G.; Trudinger, N.S. (1998): *Elliptic partial differential equations of second order.* Springer–Verlag
[10] Gilquin, H.; Laurens, J.; Rosier, C. (1993): Multi-dimensional Riemann problems for linear hyperbolic systems II. *Proc. of the 4th Intern. Conf. on Hyperbolic Problems,* Vieweg. Notes Numer. Fluid Mech. **43**, 284-290
[11] Gilquin, H.; Laurens,J.; Rosier, C. (1996): Multi-dimensional Riemann problems for linear hyperbolic systems. M^2AN **30(5)**, 527-548
[12] Ladyzhenskaya, O.A.; Ural'tseva, N.N. (1968): *Linear and Quasilinear Equations.* English Transl., Academic Press
[13] Lax, P.D.; Phillips, R.S. (1960): Local boundary conditions for dissipative symmetric linear differential operators. *Comm. Pure Appl. Math.* **XIII**, 427-455
[14] LeVeque, R.J. (1997): Wave propagation algorithms for multi-dimensional hyperbolic systems. *J. Comp. Phys.* **131**, 327-353.
[15] Li, J.; Zhang, T.; Yang, S. (1998): *The Two–Dimensional Riemann problem in Gas Dynamics.* Pitman Monographs and Surveys in Pure and Applied Mathematics 98, Longman
[16] Lukáčová-Medviďová, M.; Morton, K.W.; Warnecke, G. (1999): Finite volume evolution Galerkin methods for multidimensional hyperbolic problems. *Finite Volumes for Complex Applications II* (R. Vilsmeier et al.; eds.), 289-296. Hermès
[17] Lukáčová-Medviďová, M.; Morton, K.W.; Warnecke, G. (2000a): Evolution Galerkin methods for hyperbolic Systems in two space dimensions. *Math. Comp.* **69**, 1355–1384
[18] Lukáčová-Medviďová, M.; Morton, K.W.; Warnecke, G. (2000b): High-resolution finite volume evolution Galerkin schemes for multidimensional hyperbolic conservation laws. *ENUMATH 99, Numerical Mathematics and Advanced Applications* (Neittaanmäki, Pekka et al.; eds.), World Scientific Publishing Company, 633-640
[19] Lukáčová-Medviďová, M.; Morton, K.W.; Warnecke, G. (2000c): On high-resolution finite volume evolution Galerkin schemes for genuinely multidimensional hyperbolic conservation laws. *Proceedings of the European Congress on Computational Methods in Applied Sciences and Engineering, ECCOMAS 2000* (Oñate et al.; eds.), CIMNE 2000, 1-14
[20] Lukáčová-Medviďová, M.; Morton, K.W.; Warnecke, G. (2001): Finite volume evolution Galerkin schemes for multidimensional hyperbolic systems. *Godunov methods. Theory and applications* (E.F. Toro; ed.), Kluwer Academic / Plenum Publishers, 571-576
[21] Lukáčová - Medviďová, M.; Warnecke, G. (2000): Lax-Wendroff type second order evolution Galerkin methods for multidimensional hyperbolic systems. *East-West Journal Numer. Math.* **8(2)**, 127–152
[22] Lukáčová - Medviďová, M.; Warnecke, G., Zahaykah, Y. (1999): Evolution Galerkin methods for the multi-dimensional wave equation system. *Proceedings of the International Symposium on Electromagnetic Compatibility*, (Nitsch J. et al.; eds.), Magdeburg, 67-72
[23] Noelle, S. (1994): Hyperbolic systems of conservation laws, the Weyl equation, and multidimensional upwinding. *J. Comp. Phys.* **115**, 22-26
[24] Oleinik, O.A.; Radkevič, E.V. (1973): *Second Order Equations with Nonnegative Characteristic Form.* American Mathematical Society
[25] Ostkamp, S. (1997): Multidimensional characterisitic Galerkin schemes and evolution operators for hyperbolic systems. *Math. Meth. Appl. Sci.* **20**, 1111-1125
[26] Schulz-Rinne, C.W. (1993): Classification of the Riemann problem for two-dimensional gas dynamics. *SIAM J. Math. Anal.* **24(1)**, 76-88
[27] Smoller, J. (1982): *Shock Waves and Reaction–Diffusion Equations.* Springer–Verlag, 1982.
[28] Treves, F. (1985): *Basic Linear Differential Equations.* Academic Press
[29] Zhang, P.; Li, J.; Zhang, T. (1998): On two–dimensional Riemann problem for pressure-gradient equations of the Euler system., *Discrete and Discont. Dyn. Syst.* **4(4)**, 609-634

Received January 2001; final version October 2002.

E-mail address: jiequan@mail.cnu.edu.cn
E-mail address: lukacova@tu-harburg.de
E-mail address: Gerald.Warnecke@mathematik.uni-magdeburg.de